PROCESSES LIMITING DEPTH OF ARROYO INCISION: EXAMPLES FROM THE RIO PUERCO, NEW MEXICO

Eleanor Griffin, Research Hydrologist, U.S. Geological Survey, Boulder, CO, egriffin@usgs.gov; and Jonathan Friedman, Research Hydrologist, U.S. Geological Survey, Fort Collins, CO, friedmanj@usgs.gov

Abstract: We examined channel flow and suspended sediment transport processes within the lower Rio Puerco arroyo, located in semi-arid north-central New Mexico, in an attempt to answer the question: Why did arroyo incision stop by about 1936? Channel flow model results show that in the narrow, incised channel of 1936, the boundary shear stress during a large flood was highest over the lower banks and bank toes, causing a higher potential for erosion of these surfaces than of the channel bed. This would have caused the channel (and arroyo) to widen, and the higher sediment fluxes from those surfaces would have inhibited the capacity of the flow to erode the bed. We found that volumes of sediment delivered to the channel from local erosion of the arroyo wall did not exceed the capacity of the flow to transport sediment, including sand, in suspension. However, sediment supplied from erosion upstream of our study reach may have reduced the capacity of the flow to erode the bed. Our results suggest that arroyo incision ended with the observed reduction in flood peak magnitude, frequency, and duration after 1941.

INTRODUCTION

Channel incision in the semi-arid southwestern United States in the mid- to late-1800s through early 1900s led to the development of arroyos, which are steep-sided, narrow gullies in which flood flows no longer overtop the walls (Hovey, 1902; Bryan and Post, 1927). Arroyos created hazards for travel and to livestock, and downcutting of the channel eliminated opportunities for flow diversion for irrigation (Bryan, 1928). Large volumes of sediment transported in the Rio Puerco downstream to the mouth between 1929 and the mid-1940s contributed to channel bed aggradation and increased flooding in the middle Rio Grande (Happ, 1948; Welsh, 1985). In addition, the high rate of sediment delivery to the Rio Grande decreased storage capacity of Elephant Butte Reservoir (Figure 1; Bryan and Post, 1927).

Between 1927 and 1936, the 55-km-long lower Rio Puerco arroyo (Figure 1) both widened and incised. Large floods in 1929, 1935 and 1936 contributed to an increase in arroyo volume by about 44.5 x 10^6 m^3 during this period (Friedman et al., 2014). Average arroyo width in this reach nearly doubled, increasing from 118 m in 1927 to 212 m by 1935 (Friedman et al., 2014). In the first 10 valley km (vk) downstream from Highway 6, arroyo depth increased from an average of about 12.1 m in 1927 (Bryan, 1928) to about 14.6 m by 1936 (Friedman et al., 2014). Arroyo volume can increase either by: 1) channel bed incision; 2) block failure of an arroyo wall undercut by channel or floodplain flow; or 3) erosion of inset terraces by meander migration. Eroded sediment can be redistributed within the arroyo, but some fraction of that sediment must be transported down-valley to the mouth in order to have a net increase in arroyo volume through time. In the lower 55 km of the Rio Puerco arroyo, we know that channel bed incision continued until shortly after the flood of record in 1929 and reached a maximum near Highway 6 by about 1936 (Elliott et al., 1999; Friedman et al., 2014). Much of the sediment eroded from the arroyo walls, channel bed, or inset terraces was transported down-valley and either deposited near the mouth, forming a delta, or transported into the Rio Grande (Bryan and Post, 1927; Tuan, 1966).

We examined the processes that caused incision of the channel bed and erosion of the arroyo walls in the first 10 km down-valley from the concrete sill near the Highway 6 crossing (Figure 1). A single arroyo cross section surveyed by K. Bryan in August 1936 (Elliott et al., 1999), located at vk 0.76, provides an example of the shape of the incising arroyo and inset active channel. At this location, the arroyo depth (height of the pre-arroyo valley floor above the channel bed) increased from 13.0 m in 1927 to 15.6 m in 1936, and subsequent aggradation on the bed reduced the depth to 14.9 m by August 1972 (Elliott et al., 1999). Dated sediment deposits in a trench excavated across the arroyo bottom at vk 0.84 km (the Highway 6 trench) indicate that the arroyo bottom has been aggrading since at least the early 1960s (Friedman et al., 2014). The question we address here is: Why did incision stop by about 1936?

Background: The Rio Puerco is an ephemeral tributary of the Rio Grande incised in fine valley-fill sediment, dominantly sand, silt and clay (Heath, 1983; Love, 1986). The watershed occupies 19,040 km^2 dominated by easily eroded sedimentary rocks (Heath, 1983). Elevation ranges from 3444 m at the summit of Mount Taylor, near the

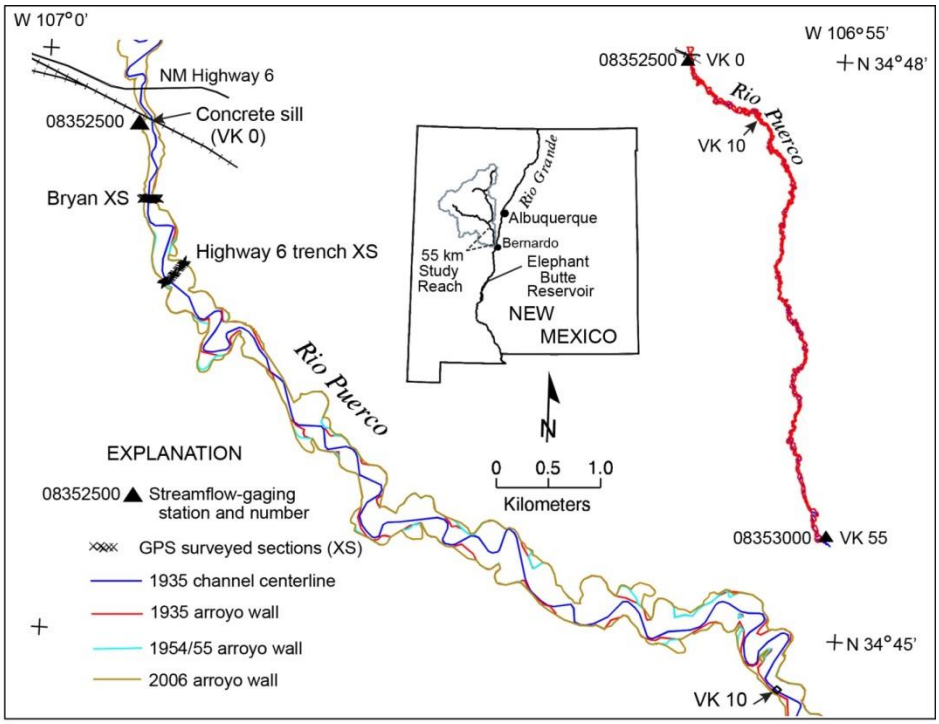

Figure 1 Map of the study reach. We focused this study on incision and arroyo wall erosion processes in the first 10 km downstream from the concrete sill on the downstream side of the railroad bridge near the Highway 6 crossing. Locations of two historical streamflow-gaging stations within the lower Rio Puerco arroyo are shown. Arroyo wall locations in 1935 (red line), the 1950s (light blue line), and 2006 (tan line) show the extent of arroyo widening since 1935. Where lines representing the 1935 and 1954/55 arroyo walls are visible, the arroyo has widened.

center of the watershed, to 1440 m at the mouth of the Rio Puerco near Bernardo (Figure 1). Floods usually are the result of sequences of summer to early fall monsoonal thunderstorms (Heath, 1983; Griffin et al., 2010). Mean annual precipitation varies from about 323 mm in the northeastern highlands to 212 mm at Bernardo, NM (1948 to 1997; Molnár and Ramírez, 2001).

Records available from the U.S. Geological Survey (USGS) streamflow-gaging stations Rio Puerco at Rio Puerco, NM (#08352500), located at vk 0 (Figure 1), and Rio Puerco near Bernardo, NM (#08353000), located at vk 55, indicate that annual peak flows have declined since the flood of record in September 1929 (Friedman et al., 2014). The magnitude of the peak flow on 23 September 1929 was 1,070 m^3/s at Rio Puerco (New Mexico State Engineer, 1930). This event was preceded by a flood with a peak discharge of 880 m^3/s in August 1929. The 1929 floods damaged the Atchison, Topeka, and Santa Fe (AT&SF) Railway Company railroad bridge at the Highway 6 crossing (Figure 1). During the bridge reconstruction in 1930, the concrete sill on the downstream side of the bridge was extended to the full width between abutments, and four concrete steps were added with a total drop from the sill to the downstream channel bed of 4.7 m (Powell, L.H., Chief Engineer, AT&SF Railway Company, written commun., 1953).

The Rio Puerco is known to carry high concentrations of sediment in suspension and to convey high suspended sediment loads (Nordin, 1963; Elliott et al., 1999; Bierman et al., 2005). More than 50% of 524 suspended sediment samples collected at the gage Rio Puerco near Bernardo between October 1947 and September 2002 had concentrations >100,000 mg/L (volume concentration (vol. conc.) > 0.0377; USGS Water-Quality data, 2014a). All samples with concentrations higher than 199,000 mg/L (vol. conc. 0.0751; n = 59) contained sand (Griffin et al., 2014).

The capacity of open channel flow to erode a surface is dependent in part on the sediment load already carried in the flow. Flow entering a reach that already is carrying the maximum sediment load cannot erode a surface unless there is an increase in the shear stress, which can be caused by a constriction in the channel or an increase in slope, for

example. In contrast, if the upstream sediment supply has been cut off by dam construction, then the magnitude of incision and widening can be extreme (Xia et al., 2014). Sand in suspension is transported at about the mean velocity of the fluid, whereas sand transported as bedload moves at the much lower velocity of the near-bed region of the flow. Suspended sediment samples collected by Nordin (1963) and annual suspended sediment loads (Elliott et al., 1999; Bierman et al., 2005) indicate that the dominant mode of sediment transport in this river is in suspension, and we assume that bedload transport is negligible.

Erosion of the Rio Puerco channel bed and arroyo walls is initiated by flow with locally increasing shear stress and increasing capacity to transport sediment, including the fine to very fine sand found in this system (Friedman et al., 2014). The process of wall erosion is dominated by undercutting of the cohesive wall by fluvial erosion along the exposed base of the wall (Figure 2). Layers of clay within the pre-arroyo valley-fill sediment provide cohesion that supports a steep wall face despite heights of more than 10 m. Field observations indicate that block mass failures occur when the wall has been undercut by 1.5 m or more. A single mass failure can deliver a large volume of sediment to the arroyo bottom. Sediment deposited on the arroyo bottom from wall mass failures temporarily protects the base of the wall from erosion. These failures also increase the local availability of sediment for transport, reducing the capacity of the flow to erode the bed.

Any geomorphic, hydrologic, or vegetative change that reduces the magnitude and duration of shear stress acting on the sediment surface can reduce the rate of incision. Possible changes include a reduction in runoff magnitude or duration through time, geomorphic changes that cause a reduction in bed gradient or an increase in flow width, or vegetative changes that add drag to the flow, reducing the shear stress on the sediment surface (see Simon et al., 2000). An increasing sediment load from erosion upstream also can reduce the capacity of flow to erode the bed.

We examined historical flow data (USGS, 2014a,b) and observed geomorphic changes in the arroyo (Friedman et al., 2014) to identify possible causes of the termination of incision in the lower Rio Puerco. We applied a physically based model for flow (Kean and Smith, 2004) to determine how observed widening of the arroyo bottom affected the boundary shear stress distribution during a large flood and the capacity of the flow to transport sediment in suspension. We compared the capacity of the flow to transport sediment with the available record of suspended sediment load transported past the gage near Bernardo (USGS, 2014a). Finally, we compared the extent of arroyo wall erosion determined from wall locations mapped from aerial imagery and LiDAR data covering the reach from vk 0 – 10 for four time intervals between 1935 and 2010.

Progression of incision and widening upstream from the study reach may have contributed to high sediment loads entering the reach, which could have limited the capacity of the flow to erode the bed in the study reach. Using available topographic data (Friedman et al., 2014), we can estimate the volumes of erosion and deposition within the

Figure 2 Example of a sharp bend in which channel flow has undercut the arroyo wall. The pre-arroyo valley-floor surface is about 10.5 m above the channel bed. The thickness of the undercut wall segment is about 7.6 m. Channel flow direction is from bottom of photo to middle left. (Photo taken April 3, 2010 by E. Griffin.)

study reach through time, but have no knowledge of volumes of sediment transported into the reach from upstream. Therefore, we can only infer the possible effects of increased incoming sediment loads on erosion of the arroyo bottom through time.

METHODS

Historical Flow and Suspended Sediment Transport: The streamflow-gaging station Rio Puerco at Rio Puerco, NM, located at the upstream end of our study reach (Figure 1), was operated from Water Year (WY) 1935 through 1976. Additional annual peak flows were determined from peak gage height and indirect discharge measurements at this station through WY 1991 (USGS, 2014b). Limited sediment data were collected at this site. The streamflow-gaging station Rio Puerco near Bernardo, NM, has been in continuous operation since WY 1941, and suspended sediment data are available beginning for WY 1956. We computed annual flow volumes at Rio Puerco for WY 1935 through 1976 and near Bernardo for WY 1941 through 2013 to examine changes through time. By the mid-1970s, the Rio Puerco channel had narrowed and woody vegetation canopy covered 47% of the arroyo bottom (Friedman et al., 2014), changing the flow distribution within the arroyo. Therefore, we applied linear regressions to determine the average relations between annual flow volume and suspended sediment load for the periods 1956 to 1975 and 1976 to 2013, and we estimated the sediment load for WY 1941 using the regression equation for the first period.

Topographic and Imagery Data Sources: Available topographic and imagery data include data from aerial Light Detection and Ranging (LiDAR) surveys conducted in April and July 2005 (Vincent et al., 2009) and March 2010 (Perignon et al., 2013). Arroyo features were mapped from imagery collected in 1935, 1954/55, 1975/79, and 2005 (Friedman et al., 2014). Bryan and Post (1927) and Bryan (1928) provided arroyo width and depth data collected in the late 1800s and early 1900s. All data have been referenced to the North American Datum of 1983 (NAD 83; horizontal datum) and to the North American Vertical Datum of 1988 (NAVD 88).

Channel Shape: Arroyo geomorphic data for the period of incision are almost entirely limited to measurements of arroyo width and depth. Channel width in 1935 determined from aerial imagery (Friedman et al., 2014) ranged from about 30 to 65 m, with an average of 41.1 m. The arroyo cross section surveyed by Bryan in August 1936 (Figure 3; Elliott et al., 1999) provides an example of the incised channel geometry near the end of the phase of incision. Top width of the inset channel in the 1936 Bryan cross section was 41.5 m, center depth was 4.6 m, cross-sectional area was 129 m^2, and the average bank angle was 20.3°.

Previous studies (Kean et al., 2009; Griffin et al., 2010) have shown that the sharp corners between the recently eroded channel bed and bank are areas of high shear stress, causing them to be short-duration, transient features. Therefore, we applied the Kean and Smith (2004) model using a channel shape similar to the 1936 Bryan cross section with a slightly rounded bank toe (**Case A**; Figure 3). We computed flow in the inset channel only, neglecting the terrace area to the right of the channel, artificially extending the banks upward in order to simulate flow in the early, narrow arroyo. For subsequent cases (B and C), we progressively widened the channel and reduced the bank angle as described below.

Nordin's (1963) cross sections surveyed in August and September 1961 near vk 55 provide examples of the channel that widened after initial incision. **Case B** is the channel shape from Case A, widened to match the width of the channel surveyed by Nordin (1963) on 19 August 1961, when measured discharge was 40.5 m^3/s. At a center depth of 1.89 m, top width was 35.9 m (36.5% wider than the channel shape in Case A at the same depth), cross-sectional area was 52.4 m^2, and the average bank angle was 15.3°. Again, for flow modeling purposes, the banks were extended upward at the same angle to accommodate the target flow.

Case C has the same bank geometry as Case B, but with the relatively flat segment in the center of the channel widened by 10 m. This channel shape simulates the wide, braided channel within the arroyo following the large floods of the 1930s and early 1940s (Friedman et al., 2014). Shrub canopy covered an average of only 9% of the arroyo bottom in 1935, and, in many cases, the shrubs present in 1935 were far from the channel (Friedman et al., 2014). In addition, frequent large floods between 1929 and 1936 prevented the establishment of vegetation on the channel bed (arroyo bottom). Therefore, we did not include drag on woody vegetation in these calculations.

Arroyo Wall Erosion: Erosion of the arroyo wall increases planimetric area of the arroyo, which can be used to estimate eroded sediment volumes. We mapped the 2010 arroyo wall locations from the 2010 LiDAR DTM

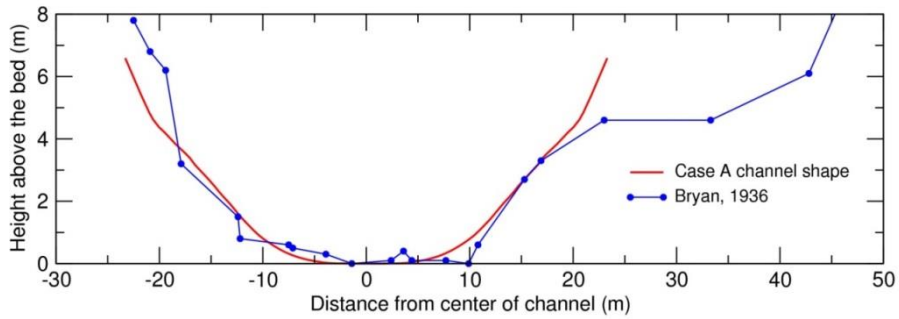

Figure 3 Initial modeled channel shape (Case A; red line), compared to the cross section surveyed by K. Bryan on 5 August 1936 (blue line; Elliott et al., 1999).

(Perignon et al., 2013) in the reach vk 0 – 10 for comparison with previously mapped wall locations in 1935, 1955, 1979, and 2005. We then mapped extents of wall erosion in each of four time intervals: from 1935 to 1955 (length = 20 yr); from 1955 to 1979 (length = 24 yr); from 1979 to 2005 (length = 26 yr); and from 2005 to 2010 (length = 5 yr). Although the last interval is considerably shorter than the others, there was a large flood within this interval (Vincent et al., 2009). For each of the four time intervals we identified: 1) average channel sinuosity; 2) the length of arroyo wall at the start of the interval exposed to channel flow at the base; 3) the length of arroyo wall at the start of the interval that was eroded by the end of the interval; 4) the total planimetric area eroded; and 5) the average wall erosion rate. The average arroyo wall erosion rate (m/yr) was computed by dividing the plan area eroded (m^2) by the length of wall eroded (m) and the number of years in the interval (yr). The computed erosion rates give the average movement of the arroyo wall through time at sites where the mapped change in wall location was >2 m (the minimum detectible movement; Friedman et al., 2014). The volume of sediment eroded from the arroyo wall between 1935 and 1955 was estimated by multiplying the eroded planimetric area by the estimated average height of the valley floor above the channel bed in 1955, about 14.4 m in this reach (Friedman et al., 2014).

Channel Flow Model Application: In a wide, unvegetated channel, the perimeter-averaged boundary shear stress, τ_b, is ρgRS, where ρ is the density of water in a clear-water flow (1,000 kg/m^3), or it is the bulk density of the fluid, ρ_f, in a sediment-laden flow, g is acceleration due to gravity (9.81 m/s^2), R is the hydraulic radius (m), and S is the water-surface slope, estimated here as the average bed slope. We assumed an average sediment density, ρ_s = 2,650 kg/m^3, and computed ρ_f using the equation

$$\rho_f = (1 - C_s)\rho_w + C_s \rho_s , \tag{1}$$

where C_s is the volume concentration of sediment in suspension and ρ_w is the density of water. We assumed that flow was quasi-steady and locally uniform in the down-valley direction and computed flow in the incised channel using the Kean and Smith (2004) model. This model includes the effects of friction on the lateral boundaries in the computation of the flow and boundary shear stress distributions. The model has been applied previously to compute flow in the narrow Rio Puerco channel of 2002 – 2007 in a reach with vegetated banks (Griffin et al., 2005) and in a reach in which bank vegetation had been killed by herbicide and removed by a flood (Griffin et al., 2010). This study is the first application of the model to compute flow in a narrow, deeply incised channel with large capacity. In all cases, the channel was assumed to be straight, with no secondary circulations in the flow.

We selected the magnitude of the annual peak discharge recorded on 23 September 1941, 480 m^3/s, as the target discharge (USGS, 2014b). This discharge is on the order of the mean annual peak flow for the record of the gage at Rio Puerco, 242 m^3/s, plus one standard deviation, 199 m^3/s (n = 51 yr). After 1941, annual peak flows exceeded 480 m^3/s only in 1972, 2006, and 2013. We applied the model to compute the depth of flow required to convey that discharge for each of the three cases for a narrow (Case A) to wide (Case C) channel.

Elevations of the channel bed determined from field survey data or estimated from trench stratigraphy near Highway 6 and Bernardo (Figure 1) combined with mapped channel centerline lengths through the 55 km-long arroyo segment indicate that an average channel bed slope of 0.0011 has been maintained through time since 1935 (Friedman et al., 2014). This slope is used for all of the calculations below. The average down-valley slope is 0.0016 (Griffin et al., 2014). Average sinuosity in 1935 was 1.33 (Friedman et al., 2014).

We assumed that channel bed roughness for flows with a meter or more depth was similar to that measured by Nordin (1963) in August and September 1961 (n = 0.014 to 0.016) and set the bed roughness, z_0, equal to 0.00016 m (Griffin et al., 2014). In a sand-bed stream, these flows are in the upper plane bed regime (Nordin, 1963; Guy et al., 1966). We estimated roughness of recently eroded banks starting 0.30 m above the bed as 0.005 m (Griffin et al., 2010). In the region of the lower bank and bank toe, we used a length-weighted average of the two values. We then calculated the depth required to convey the target discharge for each channel shape.

Computation of Suspended Sediment Transport: The capacity of the flow in the channel to transport sand and finer material in suspension was computed following the method of McLean (1992) and Smith and McLean (1977). We used the bed material distributions found by Griffin et al. (2014) to result in concentration profiles for each of 5 sediment sizes, ranging from medium silt to medium sand, that matched suspended sediment concentrations measured by Nordin (1963) on 20 September 1961 (Table 1). The transport of sand in suspension is dependent on the availability of sand for transport. Field observations (Nordin, 1963; Griffin et al., 2014) and suspended sediment measurements (USGS, 2014a) indicate that the availability of sand for transport has been highly variable through space and time. We assumed that channel bed porosity was 35%, giving a spatially averaged concentration of sediment in the bed, C_b, of 65%, and compensated for variability in availability of sand for transport by assuming sand covered only 25% of the bed in all cases (Topping et al., 2007; Griffin et al., 2014). Concentration profiles were computed for three segments of the channel flow in each case: 1) the middle of the channel over the nearly flat bed; 2) the lower bank and bank toe; and 3) the upper bank. We used the model-calculated τ_b distribution to determine the average τ_b in each segment, specified flow depth as the average depth in the segment, and computed the unit width sediment and sand fluxes (q_s and q_{sand}) in each segment. The total sediment and total sand fluxes in each case were computed by summing the fluxes in each segment.

In the absence of vegetative drag and form drag on topographic roughness elements, the skin friction shear stress, τ_{sf}, needed to compute the sediment transport, is equal to τ_b. Sediment is carried into suspension by turbulent diffusion, and the transport of sediment in suspension is determined by the ratio of the shear velocity, u_*, = $(\tau_b / \rho_f)^{1/2}$, to the sediment settling velocities (Yalin, 1972; Smith and McLean, 1977). Settling velocities for each particle size were determined using the method of Dietrich (1982). We estimated the near-bed reference concentration, C_a, using the equation

$$C_a = \frac{\gamma_0 C_b (T_* - 1)}{1 + \gamma_0 (T_* - 1)}, \tag{2}$$

(Smith and McLean, 1977) where T_* is the transport stage, equal to τ_b / τ_{cr} , τ_{cr} is the critical shear stress for erosion of sediment of a given size, and γ_0 = 0.004 (P.L. Wiberg, reported by McLean, 1992).

The computation of suspended sediment concentration profiles required iteration in each case, as the concentration of sediment in suspension affects the bulk fluid density (equation 1), which affects the sediment settling velocity (Dietrich, 1982). For each iteration, we modified the sediment settling velocities following the method of Dietrich (1982) and recomputed the suspended sediment concentration until the bulk fluid density from the previous iteration

Table 1 Bed material distribution assumed for suspended sediment calculations.

Sediment size (mm)	Fraction of bed material	Clear-water settling velocity (m/s)	Settling velocity with ρ_f = 1130 kg/m^3 (m/s)
0.016	0.40	0.00020	0.00015
0.050	0.14	0.0020	0.0015
0.065	0.20	0.0032	0.0025
0.13	0.19	0.0102	0.0081
0.26	0.07	0.0267	0.0231

was within 5% of the output bulk fluid density. Examples of the decrease in settling velocity for each grain size are shown in Table 1 for ρ_f = 1,130 kg/m^3 (vol. conc. 0.079).

Change in bed elevation (η) with time (t) is calculated from the 1-dimensional sediment continuity equation:

$$\frac{\partial \eta}{\partial t} = -\frac{1}{C_b}\left(\frac{\partial q_s}{\partial x}\right), \tag{3}$$

where x is distance downstream. Erosion of the bed can occur when there is an increase in the sediment flux through time, as during the rising limb of a flood, or with distance downstream. However, the capacity of a flow to erode the bed is strongly dependent on the sediment concentration already in suspension in the flow, which we cannot determine for the early 1900s floods in the study reach.

High concentrations of sand in suspension can cause a density gradient that dampens the turbulent mixing (Gelfenbaum and Smith, 1986; McLean, 1992). Data from Nordin (1963) and our field observations (Griffin et al., 2010) suggest that topographic irregularities in the Rio Puerco inhibit the development of a stable density-stratified flow, and we neglect that process here.

RESULTS

Annual Flow Volume and Suspended Sediment Load: Annual flow volumes from both gages (Figure 4) show a declining trend through time. Continuous flow data are not available for 1929, but the combined August and September flood magnitudes suggest that flow volume in that year was likely higher than in any year of the record. Floods in 1935 and 1936 produced high runoff volumes, but the largest flow volume in the period of record was in WY 1941, when high rainfall caused floods in May, September, and October (Heath, 1983). During the period of overlap in operation of the two gages from WY 1941 to 1976, the volume measured at Bernardo was an average of 94% of the volume measured at the upstream gage. Suspended sediment data from the gage near Bernardo also show a declining trend through time (Figure 5), with the relation between annual suspended sediment load and annual flow volume returning a higher load for a given flow volume in WY 1956 to 1975 than for the same flow volume in WY 1976 to 2013. Extrapolation of the regression for the early period to estimate flow volume in WY 1941 gives a total sediment load of 16.9 x10^6 metric tons (t), about the same as that in WY 1957.

Comparing the average annual sediment load for the period WY 1956 to 1975, 5.05 x 10^6 t/yr (sd = 2.80 x 10^6 t/yr; n = 19) to that for the period WY 1976 to 2013, 1.64 x 10^6 t/yr (sd = 1.01 x 10^6 t/yr; n = 37) shows a 66% decrease in the average annual load. Average annual flow volume also decreased, but only by 37%, from 40.0 x 10^6 m^3/yr (sd = 29.1 x 10^6 m^3/yr; n = 19) to 25.3 x 10^6 m^3/yr (sd = 19.3 x 10^6 m^3/yr; n = 37).

Channel Flow, Boundary Shear Stress, and Suspended Sediment Transport: Channel flow model results for **Case A** (Figure 6) show that as stage (center depth), h, increases from 1.10 to 5.10 m, the τ_b distribution changes from being relatively uniform across the bed and lower banks to showing areas of high stress over the bank toe and lower bank. Discharge increases from 33.0 m^3/s at h = 1.10 m to 480 m^3/s at h = 5.10 m, and the perimeter-averaged τ_b increases from 8.9 to 36.3 N/m^2. When h = 1.10 m, the model-calculated τ_b in the center of the channel is the same as ρghS. As flow depth increases, the difference between τ_b and ρghS in the middle of the channel increases, with a 30% difference between the two values when h = 5.10 m.

At h = 5.10 m, the average τ_b in the 7-m-wide zone of high stress over the bank toe is 51.5 N/m^2, 43% higher than the average in the middle of the channel, 35.9 N/m^2 (Figure 7A). The computed volume concentration of sediment in suspension, 0.0829, gives a total sediment flux of 39.8 m^3/s, and the computed sand flux is 13.4 m^3/s (Table 2). If the flow discharge were sustained at 480 m^3/s for one day and an unlimited supply of sediment, including sand, were readily available for transport, then the total sediment volume transported in a day could have been 3.44 x 10^6 m^3, and the sediment load could have been 9.11 x 10^6 t.

Flow depth in the wider channel of **Case B** required to convey 480 m^3/s is 4.16 m, 18% less than the depth in Case A. The maximum τ_b is reduced by 18%, and the difference between the average τ_b over the bank toe and τ_b in the

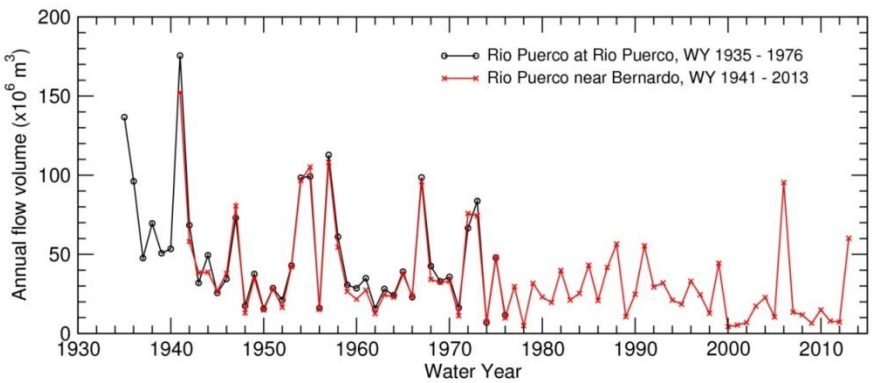

Figure 4 Annual flow volumes at the streamflow-gaging stations Rio Puerco at Rio Puerco (#08352500) and Rio Puerco near Bernardo, NM (#08353000). Declining trends in annual flow volumes are correlated with declining trends in annual peak flows.

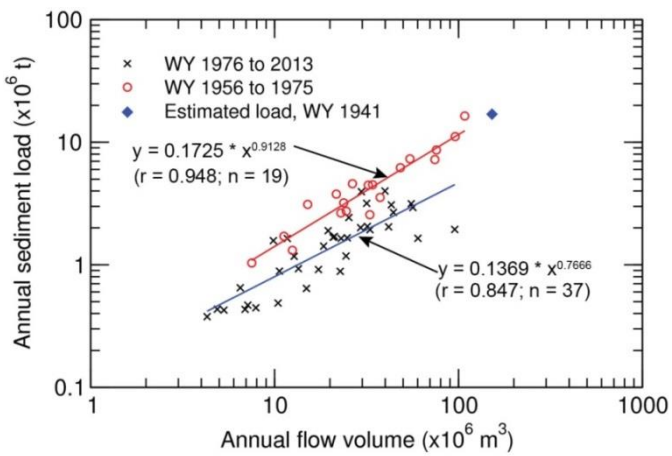

Figure 5 Annual sediment load as a function of annual flow volume from the record of the gaging station Rio Puerco near Bernardo, NM. Red circles are data for WY 1956 (the start of the sediment record) through 1975. Black xs are data for WY 1976 to 2013. The blue diamond is an estimate of the sediment load for WY 1941 based on the regression for WY 1956 through 1975 (red line).

middle of the channel is reduced by 17% (Figure 7). The computed τ_b in the middle of the channel is 11% less than the value of ρghS. The total sediment flux in this channel, 38.0 m^3/s, and sand flux, 12.7 m^3/s, are only 5% less than the computed fluxes in Case A (Table 2).

In the final example, **Case C**, the flow depth required to convey 480 m^3/s is reduced to 3.61 m, 29% less than depth in Case A, and the τ_b distribution approaches the more uniform pattern over the lower banks and bed, similar to the low-flow example of Case A. The maximum τ_b is 29% less than that in Case A, the average τ_b over the bank toe, 38.4 N/m^2, is only 11% greater than the average τ_b in the middle of the channel, and τ_b in the middle of the channel is only 4% less than ρghS. The total sediment flux is only 6.8% less than that in Case A, and the sand flux is 8.2% less (Table 2). The maximum τ_b in the middle of the channel is nearly the same in all 3 cases (Figure 7), ranging from 37.4 N/m^2 in Case C to 39.8 N/m^2 in case B despite the differences in flow depth.

The maximum q_s and q_{sand} (Table 2) are in the region of high τ_b over the lower bank and toe in each case. The maximum unit width fluxes are highest in the narrow channel and lowest in the wide channel, with q_s 24% lower and q_{sand} 27% lower in Case C than in Case A.

<u>Wall Erosion:</u> The extent of wall erosion from one point in time to another is related to the extent of unprotected arroyo wall exposed to channel flow at the start of the time interval (Table 3). In the reach from vk 0 to 10, the total

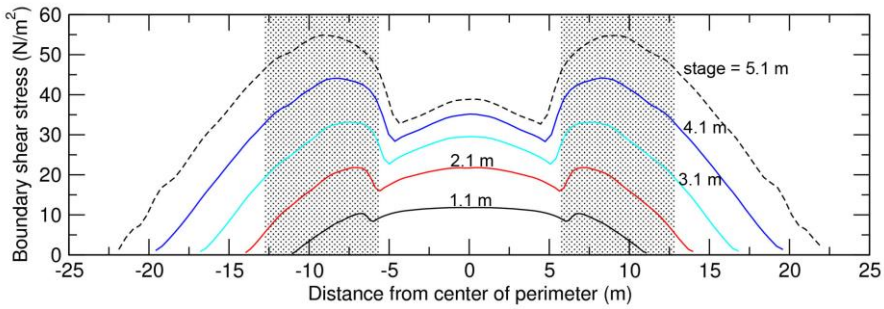

Figure 6 Change in boundary shear stress distribution with increasing flow stage from 1.1 to 5.1 m, Case A channel shape. The shading indicates areas of shear stress over the lower bank and toe.

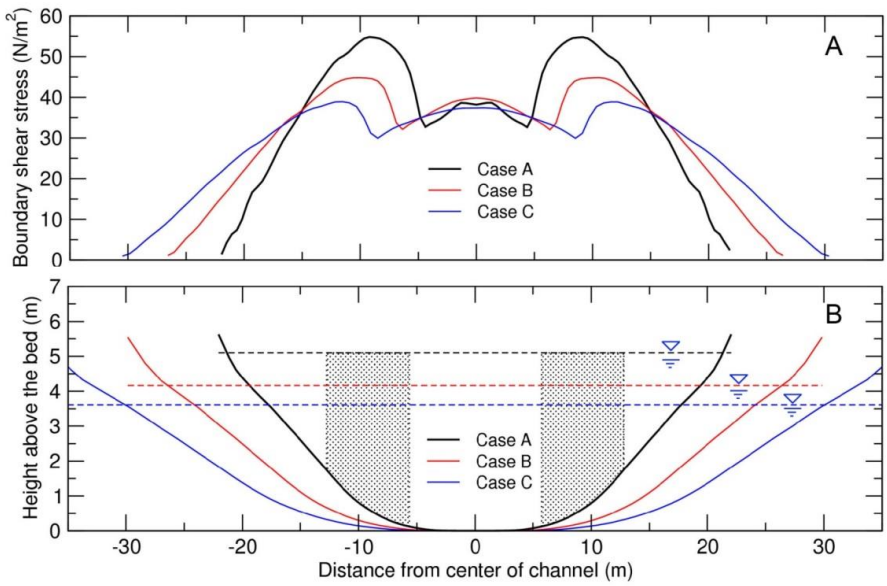

Figure 7 Model-calculated boundary shear stress (**A**) and channel shapes (**B**), with flow center depths that resulted in model-calculated discharge of 480 m^3/s. The shaded areas in B are the regions of high shear stress over the bank toe and lower bank in Case A.

length of wall segments exposed to channel flow at the base decreased from more than 6.3 km in 1935 to about 1 km by 1979. The total length of arroyo wall segments in 1935 that were eroded by 1955 was 7.9 km. Average arroyo width increased in this reach from 222 m in 1935 to 242 m by 1955. Multiplying the increase in arroyo area by the estimated height of the valley floor above the channel bed in 1955, 14.4 m, gives a volume of 2.85 x 10^6 m^3 eroded from the arroyo walls in this segment between 1935 and 1955. Assuming 35% porosity, the sediment volume eroded would have been about 1.85 x 10^6 m^3, with a total weight of 4.91 x 10^6 t, an average of 0.25 x 10^6 t/yr.

Despite the large decreases through time in annual flow volume and length of the arroyo wall exposed to channel flow at the base, the computed average wall erosion rates at sites that eroded all fall within a narrow range, from a minimum of 1.25 m/yr between 1935 and 1955 to a maximum of about 2.00 m/yr between 1979 and 2005.

DISCUSSION AND CONCLUSIONS

In all of the modeled flow cases, τ_b was above τ_{cr} for fine sand (D = 0.13 mm), 0.127 N/m^2. At the minimum modeled flow depth, h = 1.10 m, the perimeter-averaged τ_b, 8.9 N/m^2, was greater than that required to break up the clay armoring layer of the channel bed during Nordin's (1963) measurements (between 3.2 and 7.6 N/m^2). Therefore, all of the modeled flows potentially had the capacity to erode the arroyo bottom. Increasing the flow depth to 5.10 m in Case A resulted in an average shear stress over the lower bank and toe that was 43% higher than τ_b in the middle of the channel. Widening the channel reduced τ_b over the lower bank and toe so that by Case C,

with h = 3.61 m, τ_b over the lower bank and toe was only 11% greater than the average τ_b in the middle of the channel. The suspended sediment transport capacity of the 480 m^3/s channel flow was a maximum of 39.8 m^3/s in Case A. Despite a 26% reduction in mean τ_b from Case A to Case C, the capacity of the flow to transport sediment in suspension was reduced by only 7%.

The boundary shear stress distributions for Cases A, B, and C give an indication of the likely patterns of erosion during rising flow stage. The unit width sediment flux (q_s) varies with τ_b and h across the channel, and in all three cases, is maximum over the lower bank and toe (Table 2). However, the maximum q_s decreases by 24% as the channel widens from Case A to C, decreasing the potential for erosion (equation 3). During the rising limb of a flood, if the incoming sediment load is not at the capacity of the flow, increasing shear stress with stage would erode the wider channel (Case C) relatively uniformly across the bed. As stage rises in the incised, narrow channel (Case

Table 2 Channel flow and suspended sediment model results.

Parameter	Case		
	A	B	C
Center depth (m)	5.10	4.16	3.61
Average depth (m)	3.51	2.89	2.57
Top width (m)	42.7	52.4	60.1
XS area (m^2)	150.0	151.3	153.6
P (m)	44.6	53.7	60.8
R (m)	3.37	2.82	2.53
Mean τ_b (N/m^2)	36.3	30.5	27.0
Max τ_b (N/m^2)	54.8	44.8	38.9
Mean u (m/s)	3.20	3.17	3.12
Mean u_* (m/s)	0.191	0.175	0.164
Manning's n	0.0232	0.0210	0.0197
C_s	0.0829	0.0791	0.0773
C_{sand}	0.0279	0.0264	0.0257
$(q_s)_{max}$ (m^3/s)	1.19	0.99	0.90
$(q_{sand})_{max}$ (m^3/s)	0.41	0.34	0.30
Q_{total} (m^3/s)	480	480	480
Q_s (m^3/s)	39.8	38.0	37.1
Q_{sand} (m^3/s)	13.4	12.7	12.3

Table 3 Changes in arroyo wall erosion through time, vk 0 – 10.

Parameter	Time interval			
	1935 – 1955	1955 – 1979	1979 – 2005	2005 - 2010
Average sinuosity:	1.39	1.47	1.45	1.42
Length of wall exposed to channel flow at start of interval (m):	6,320	4,060	1,020	910
Length of wall at start of interval that eroded by end of interval (m):	7,900	3,210	1,410	450
Plan area eroded (m^2):	198,000	107,000	73,200	2,830
Average wall erosion rate at sites of erosion (m/yr):	1.25	1.39	2.00	1.26
Average arroyo width (m):	222	242	251	257

A), the much higher τ_b over the lower banks and toes would cause erosion of those surfaces at a higher rate than the bed. Higher concentrations of sediment over the lower banks and toe would give rise to a concentration gradient toward the center of the channel, causing mixing of the suspended sediment across the channel and inhibiting the capacity of the flow to erode the bed.

The estimated increase in volume of the lower Rio Puerco arroyo through both incision and widening between 1927 and 1935, 44.5 x 10^6 m^3 (Friedman et al., 2014), contained an estimated sediment volume of 28.9 x 10^6 m^3, or about 76.7 x 10^6 t. This total provides an average load of 9.6 x 10^6 t/yr, which is less than the estimated sediment load for WY 1941 (16.9 x 10^6 t/yr). The calculated potential sediment load for a single day of flow at 480 m^3/s in Case A, 9.11 x 10^6 t, is nearly the same as the average annual sediment load from 1927 to 1935. The sediment eroded from the arroyo walls between 1935 and 1955 in the reach from vk 0 – 10, an average of 0.25 x 10^6 t/yr, was only 5% of the average annual sediment load measured at the gage near Bernardo between 1956 and 1975 (5.05 x 10^6 t/yr). The results suggest that the suspended sediment load in the Rio Puerco often has been less than the capacity of the flow to transport sediment in suspension. Therefore, total sediment transport capacity in this system does not appear to have limited the capacity for incision.

The large reduction in length of wall segments exposed to channel flow (Table 3) was the result of increasing width of the arroyo bottom, increasing channel sinuosity, decreasing channel width after the 1940s, and increasing density of woody vegetation on the arroyo bottom through time (Friedman et al., 2014). The greater length of arroyo wall eroded from 1935 to 1955 than the length of wall exposed to channel flow in 1935 was in part the result of rapid channel migration down-valley, with average rates of up to 12 m/yr found by Friedman et al. (2014). The results indicate that arroyo wall erosion rates at sites of erosion averaged about 1.5 m/yr from 1935 to 2010. Although the trend in annual flow volume decreased through time, narrowing of the channel through time (Friedman et al., 2014) caused an increase in flow depth and τ_b as a function of discharge. In addition, sites of wall erosion between 2005 and 2010 were dominantly within sharp bends, where secondary circulations increased the shear stress along the outside of the bend, at the base of the arroyo wall (Engel and Rhoads, 2012). These changes appear to have compensated for the reduction in flow magnitude and volume through time.

The above results indicate that changes in the total suspended sediment transport capacity through time did not limit the capacity for incision. Instead, increased boundary shear stress over the lower bank and toe caused by friction on the lateral boundaries of the narrow, incised channel of 1936 would have contributed to a tendency to widen the channel (and arroyo) rather than further incise the bed. The decreasing flood peak magnitude, frequency and duration after 1941 also decreased the capacity for erosion in this system. A period of moderately low flows from WY 1948 through 1952 (Figure 4) may have provided an opportunity for widespread establishment of woody vegetation on the arroyo bottom, creating drag on future flows and a further reduction of τ_{sf} and potential to erode the bed.

Acknowledgments: The Pueblo of Isleta generously enabled the research to be conducted on their land and provided valuable historical information. Any use of trade, firm, or product names is for descriptive purposes only and does not imply endorsement by the U.S. Government.

REFERENCES

Bierman, P.R., Reuter, J.M., Pavich, M., Gellis, A.C., Caffee, M.W., and Larsen, J. (2005). "Using cosmogenic nuclides to contrast rates of erosion and sediment yield in a semi-arid, arroyo-dominated landscape, Rio Puerco Basin, New Mexico," Earth Surface Processes and Landforms, 30, pp 935-953.

Bryan, K. (1928). "Historic evidence on changes in the channel of Rio Puerco, a tributary of the Rio Grande in New Mexico," Journal of Geology, 36, pp 265-282.

Bryan, K., and Post, G.M. (1927). "Erosion and control of silt on the Rio Puerco, New Mexico," Report to the Chief Engineer, Middle Rio Grande Conservancy District, Albuquerque, New Mexico.

Dietrich, W.E. (1982). "Settling velocity of natural particles," Water Resources Research, 18(6), pp 1615-1626.

Elliott, J.G., Gellis, A.C., and Aby, S.B. (1999). "Evolution of arroyos: Incised channels of the southwestern United States," in Darby, S.E., and Simon, A., (eds.), Incised River Channels. Wiley, Chichester, UK, pp 153-185.

Engel, F.L., and Rhoads, B.L. (2012). "Interaction among mean flow, turbulence, bed morphology, bank failures, and channel planform in an evolving compound meander loop," Geomorphology, 163-164, pp 70-83.

Friedman, J.M., Vincent, K.R., Griffin, E.R., Scott, M.L., Shafroth, P.B., and Auble, G.T. (2014). "Processes of arroyo filling in northern New Mexico, USA," GSA Bulletin (in press).

Gelfenbaum, G. and Smith, J.D. (1986). "Experimental evaluation of a generalized suspended-sediment transport theory," in Knight, R.J. and McLean, J.R., (eds.), Shelf Sands and Sandstones, Canadian Society of Petroleum Geologists, Memoir II, pp 133-144.

Griffin, E.R., Kean, J.W., Vincent, K.R., Smith, J.D., and Friedman, J.M. (2005). "Modeling effects of bank friction and woody bank vegetation on channel flow and boundary shear stress in the Rio Puerco, New Mexico," Journal of Geophysical Research, 110, F04023.

Griffin, E.R., Smith, J.D., Friedman, J.M., and Vincent, K.R. (2010). "Progression of streambank erosion during a large flood, Rio Puerco arroyo, New Mexico," Proc. of the 2nd Joint Federal Interagency Conference, Las Vegas, NV, June 27 – July 1, 2010, 12 p.

Griffin, E.R., Perignon, M.C., Friedman, J.M., and Tucker, G.E. (2014). "Effects of woody vegetation on overbank sand transport during a large flood, Rio Puerco, New Mexico," Geomorphology, 207, pp 30-50.

Guy, H.P., Simons, D.B., and Richardson, E.V. (1966). "Summary of alluvial channel data from flume experiments, 1956-1961," U.S. Geological Survey Professional Paper 462-I, 96 p.

Happ, S.C. (1948). "Sedimentation in the Middle Rio Grande Valley, New Mexico," Bulletin of the Geological Society of America, 59, pp 1191-1216.

Heath, D.L. (1983). "Flood and recharge relationships of the lower Rio Puerco, New Mexico," New Mexico Geological Society Guidebook, 34th Field Conference, Socorro Region II, pp 329-336.

Hovey, E.O. (1902). "New York Academy of Sciences, Section of Geology and Mineralogy," Science, 15(384), pp 744-747.

Kean, J.W., and Smith, J.D. (2004). "Flow and boundary shear stress in channels with woody bank vegetation," in Bennett, S., and Simon, A., (eds.), Riparian Vegetation and Fluvial Geomorphology. American Geophysical Union Water Science and Application Monograph 8, pp 237-252.

Kean, J.W., Kuhnle, R.A., Smith, J.D., Alonso, C.V., and Langendoen, E.J. (2009). "Test of a method to calculate near-bank velocity and boundary shear stress," Journal of Hydraulic Engineering, 135(7), pp 588-601.

Love, D.W. (1986). "A geological perspective of sediment storage and delivery along the Rio Puerco, central New Mexico," in Hadley, R.F., (ed.), Drainage Basin Sediment Delivery. Institute of Hydrology, IAHS Publication 159, pp 305-322.

McLean, S.R. (1992). "On the calculation of suspended load for noncohesive sediments," Journal of Geophysical Research, 97(C4), pp 5759-5770.

Molnár, P. and Ramírez, J.A. (2001). "Recent trends in precipitation and streamflow in the Rio Puerco basin," Journal of Climate, 14(10), pp 2317-2328.

New Mexico State Engineer (1930). "The September flood," New Mexico State Engineer, Ninth Biennial Report, vol. 9, pp 257-264.

Nordin, C.F., Jr. (1963). "A preliminary study of sediment transport parameters, Rio Puerco near Bernardo, New Mexico," U.S. Geological Survey Professional Paper 462-C, 21 pp., U.S. Government Printing Office, Washington, D. C.

Perignon, M.C., Tucker, G.E., Griffin, E.R., and Friedman, J.M. (2013). "Effects of riparian vegetation on topographic change during a large flood event, Rio Puerco, New Mexico, USA," Journal of Geophysical Research: Earth Surface, 118, pp 1193-1209.

Simon, A., Curini, A., Darby, S.E., and Langendoen, E.J. (2000). "Bank and near-bank processes in an incised channel," Geomorphology, 35, pp 193-217.

Smith, J.D., and McLean, S.R. (1977). "Spatially averaged flow over a wavy surface," Journal of Geophysical Research, 82(12), pp 1735-1746.

Topping, D.J., Rubin, D.M., and Melis, T.S. (2007). "Coupled changes in sand grain size and sand transport driven by changes in the upstream supply of sand in the Colorado River: Relative importance of changes in bed-sand grain size and bed-sand area," Sedimentary Geology, 202, 538-561.

Tuan, Y.F. (1966). "New Mexican gullies: A critical review and some recent observations," Annals of the Association of American Geographers, 56, pp 573-597.

U.S. Geological Survey (2014a). National Water Information System, water-quality database, accessed 06/20/2014 at http://nwis.waterdata.usgs.gov/usa/nwis/qwdata.

U.S. Geological Survey (2014b). National Water Information System (NWISWeb): U.S. Geological Survey database accessed 9/16/2014 at http://waterdata.usgs.gov/nm/nwis/.

Vincent, K.R., Friedman, J.M., and Griffin, E.R. (2009). "Erosional consequence of saltcedar control," Environmental Management, 44, pp 218-227.

Welsh, M. (1985). "The United States Corps of Engineers in the Middle Rio Grande Valley, 1935-1955," New Mexico Historical Review, 60(3), pp 295-316.

Xia, J., Xiaojuan, L., Li, T., Zhang, X., and Zong, Q. (2014). "Response of reach-scale bankfull channel geometry to the altered flow and sediment regime in the lower Yellow River," Geomorphology, 213, pp 255-265.

Yalin, M.S. (1972). Mechanics of Sediment Transport, Pergamon Press, Oxford, UK.